Electronic Supplementary Information

Surface enhanced Raman scattering (SERS) in the visible range on scalable aluminum-coated platforms

Manuel Gómez,[1,2] Shima Kadkhodazadeh,[3] Massimo Lazzari[1,2]*

1 Departamento de Química Física, Facultade de Química, Universidade de Santiago de Compostela, 15782 Santiago de Compostela, Spain

2 Centro Singular de Investigación en Química Biolóxica e Materiais Moleculares (CIQUS), Universidade de Santiago de Compostela, 15782 Santiago de Compostela, Spain

3 Danchip/Center for Electron Nanoscopy (CEN), Technical University of Denmark, Kgs. Lyngby 2800, Denmark

* massimo.lazzari@usc.es

Experimental details

Fabrication of substrates

Substrates were fabricated by ultraviolet nanoimprint lithography (UV-NIL) using a commercial submicrometer-sized surface, traded by Renishaw diagnostics as Klarite®, as master mould. It consists of a square lattice of inverted square pyramidal pits with a 2.13 µm pitch, 1.46 µm side and 0.8 µm depth over a 5 x 5 mm dice of (100) silicon wafer, coated with an uniform layer of gold. Inverted replica (positive pyramidal arrays) were produced through a two-step NIL protocol where the first liquid polymer material was the two component heat-curing Sylgard 184 (Dow Corning), cured at 80ºC for two hours. The neat silicone replica was then used without further treatment as secondary mould to fabricate the direct replica of the master mould, and filled with a drop (< 10 µL) of a liquid UV-curable elastomeric polymer, either a specially synthesized tetraurethane acrylate perfluoropolyether derivative[1] or an organic modified ceramic Ormocer (Microresist Technology). Glass (1 mm thick) or PET film (100 µm thick) were used as both supporting material and planar back surface. A mask aligner with a UV-light source based on LEDs (Midas System MDA 400LJ) was used as radiation source (beam wavelength filtered for *i*-line=365 nm, intensity 20 mW cm^{-2}) with a 2-6 s exposure time. Polymeric positive pyramid arrays were obtained by exposure of the elastomeric UV-curable polymer onto the master mould.

Polymeric replicas were coated with Al by thermal evaporation (Balzers 350) at 2.5 x10^{-5} torr with a deposition rate of 50 Å s^{-1}, measured with a quartz microbalance. The quality of the polymeric replicas, in terms of dimensional variability with respect to the master mould, presence of defects and long range homogeneity, was checked by optical microscopy, high resolution field emission scanning microscopy (HR-FESEM Zeiss Ultra-Plus), high resolution transmission electron microscopy (HRTEM Jeol Jem ARM 200cF, with a spatial resolution of 0.2 nm at 120 kV) and AFM (Park XE7) operating in non-contact mode. A silicon microcantilever with the reflective side coated with aluminium (force constant 20N/m and resonance frequency of 265 kHz) and conical silicon tips was used. See additional images in Fig. S1 and S3.

Optical measurements

Reflectance spectra were recorded with an Agilent Cary 300 UV-Vis spectrometer equipped with an integration sphere accessory (Labsphere DRA-CA-301 Sphere) composed of an optical bench with double beam optics in combination with a 70 mm diameter integrating sphere coated with Spectralon® material. A first-side mirror made of glass and coated with aluminium was used as reference. Reflectance measurements were also confirmed in the wavelength range 360-740 nm by using a Konica Minolta CR-400 colorimeter operating with an 8 mm diameter measurement area.

Raman spectroscopy

Raman experiments were carried out in a Raman Spectrometer Renishaw InVia Flex, equipped with two continuous wave lasers emitting at 785 nm and 514 nm, with gratings of 1200 and 1800 lines mm^{-1}, respectively, and a Renishaw CCD 576 x 400 pix detector. All the measurements were carried out with a long 0.50 NA NPlan long working distance objective (Leica 566036), and operating with a 65 µm slit opening. Most of the measurements were carried out with a 10 s accumulation and 1% laser power, corresponding to 0.09 mW for the 514 nm laser and 9 mW for the 785 nm laser. Measurements were repeated several times for any concentration and found limited variation of peak intensity (< 15%), eventually ascribed to either structural defects or inhomogeneous deposition of the analyte. Additional spectra are shown in Fig. S4-S9.

Enhancement factor calculation

SERS enhancement factors (EF) of rhodamine 6G (R6G) and coumarin 440 were obtained for positive and inverted pyramids substrates illuminated with 514 or 785 nm laser. EFs were calculated by comparing the characteristic Raman peak of R6G at 1511 cm^{-1} or the peak of coumarin at 1162 cm^{-1}, at the concentration 1 x 10^{-6} M. Normal Raman references were obtained directly from the corresponding ethanol solution deposited onto a silicon wafer.

The experimental EF is given by the equation:[2]

$EF= (I_{SERS}/N_{SERS}) /(I_{Raman}/N_{Raman})$

where I_{SERS} and I_{Raman} are the SERS and normal Raman intensities, respectively, of the characteristic peaks, measured as integrated number of counts (area under the band); N_{SERS} is the number of molecules contributing to the SERS signal, calculated taking into account the area of the excitation laser spot (24 µm x 2.5 µm for the 785 nm laser, and circular with 4.2 µm diameter for the 514 nm laser), the concentration and the total amount of the deposited solution; and N_{Raman} is the number of molecules within the excitation volume calculated on the basis of the laser spot area, the depth reached by the laser light and the solution concentration. Calculated values are shown in Table S1.

FDTD simulations

In order to simulate the reflection properties of the substrates and their field accumulation we used a commercial package (Lumerical FDTD Solutions) that solves the Maxwell´s equations for structures in the range of the wavelength of the radiation used. In particular, it can be used to study plasmonic effects of micro and nanoscale metal structures and allows simulating the field distribution and visualizing the local field enhancement associated to the grating structure. The workflow consists in building the 3D model of the structures where only a single unit cell is required (a periodic boundary approximation solution for this single unit cell is developed assuming it is placed in an infinitely large array), setting the simulation parameters (material, mesh, boundary conditions and time), defining the light sources and the monitors to register the field change with time, and finally running the simulation and optimize the results.

The systems were simulated by building a unit consisting in a whole pyramid or pyramidal well and half of the corridor around it, and considering the presence of a 150 nm Al layer. As boundary conditions in the z direction, we used Perfect Matching Layers (PML) that act as absorbers for non-periodic directions. As light source, a normal to the substrate incident plane wave was used, having a Gaussian pulse in time domain. The plane wave was a Field/Scattering Field (TFSF), which allows subtracting the incident field, so only scattered fields propagate. Monitors were placed both in the horizontal and vertical positions to have a more precise picture of spatial field distribution.

EELS spectroscopy

EELS measurements were carried out in a monochromated FEI Titan instrument in STEM mode operated at 120 kV. The spatial and energy resolution of the measurements were 0.5 nm and 0.15 eV, respectively. Spectrum images with pixels sizes of 10-15 nm from areas with dimensions 2000 nm x 2000 nm were acquired to map the surface plasmon resonances supported by the pyramid structures. An acquisition time of 50 ms per pixel was used. The spectra were analyzed after removing the zero-loss peak (ZLP), using a power law model to fit the positive energy tail of the ZLP. The surface plasmon resonances present in the data were fitted with a Gaussian function to determine the energy of their maxima.

References

1. M. Gómez and M. Lazzari, *Microelectron. Eng*., 2012, **97**, 208.
2. E.C. Le Ru, E. Blackie, M. Meyer and P.G. Etchegoin, *J. Phys. Chem. C*, 2007, **111**, 13794.

Table S1. Calculated EFs of target analytes for 150 nm Al-coated positive and inverse pyramids substrates illuminated with 514 or 785 nm laser.

Analyte	Substrate pyramid type	Excitation wavelength (nm)	EF[a]
R6G	inverse	514	5.5×10^9
	positive	514	1.7×10^8
	inverse	785	2.2×10^7
	positive	785	3.4×10^6
Coumarin	inverse	514	3.6×10^7
	positive	514	6.1×10^6
	inverse	785	3.6×10^7
	positive	785	6.1×10^6

[a] The area of the peaks at 1511 and 1162 cm^{-1} were used for the calculation of the EFs of R6G and coumarin, respectively.

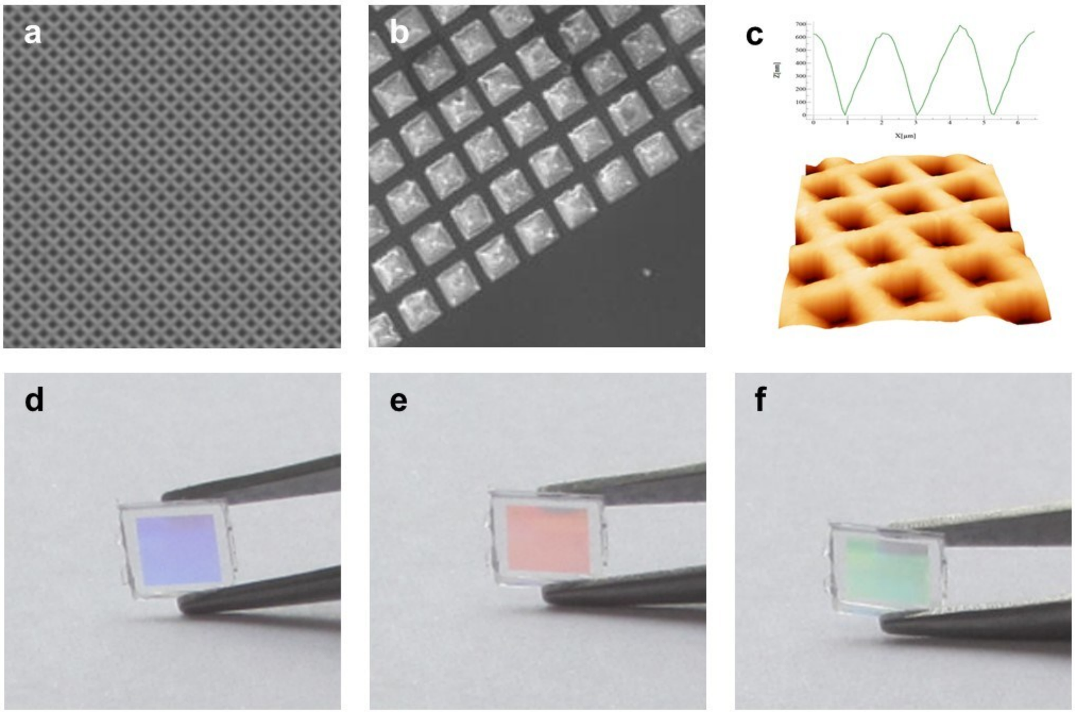

Fig. S1 SEM micrographs of Al-coated inverted (**a**) and positive pyramids (**b**) substrates, AFM profile of inverted pyramids arrays before Al coating (**c**), and photographs of 5 X 5 mm substrates with different tilting (**d-f**).

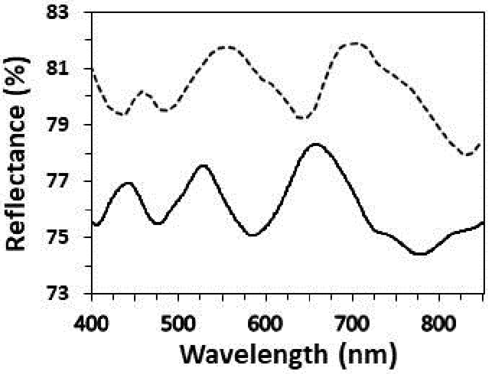

Fig. S2 Magnified reflection spectra of Al-coated inverted (solid curve) and positive (dashed curve) pyramids substrates.

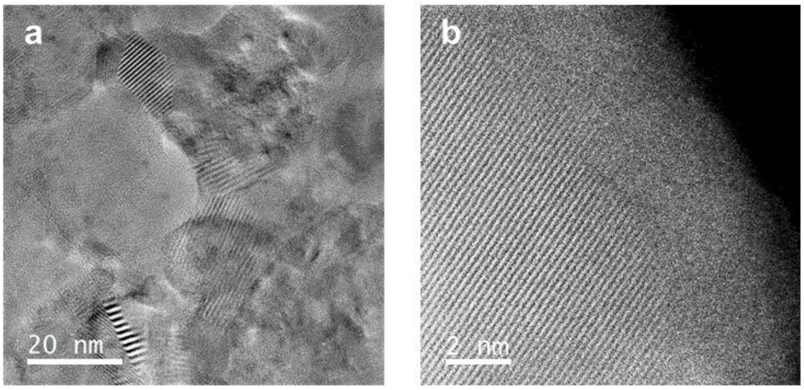

Fig. S3 Bright field TEM image of the Al layer showing the random orientation of the nanocrystals (**a**), and of the lattice fringes corresponding to the (111) plane of the fcc structure of Al with a d spacing of 2.33 Å (**b**). In the latter image an amorphous Al_2O_3 passivation layer with a thickness of around 3 nm can be seen.

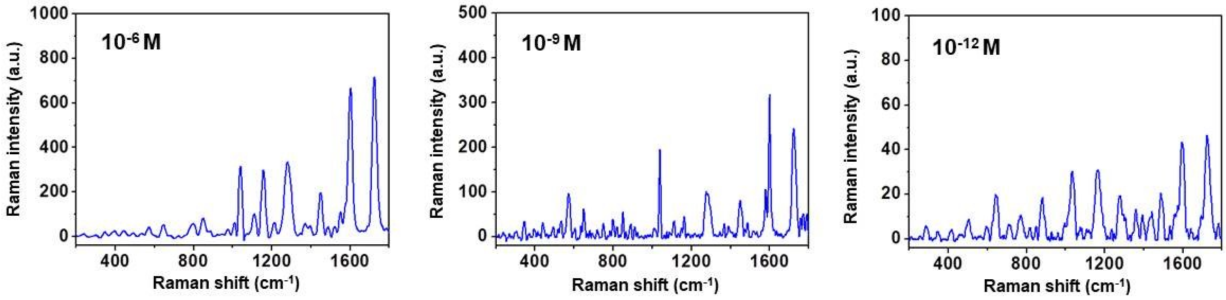

Fig. S4 Raman spectra of coumarin from solutions with different concentration at 514 nm excitation wavelength on inverted pyramids SERS device (10 s exposure time, power 0.09 mW).

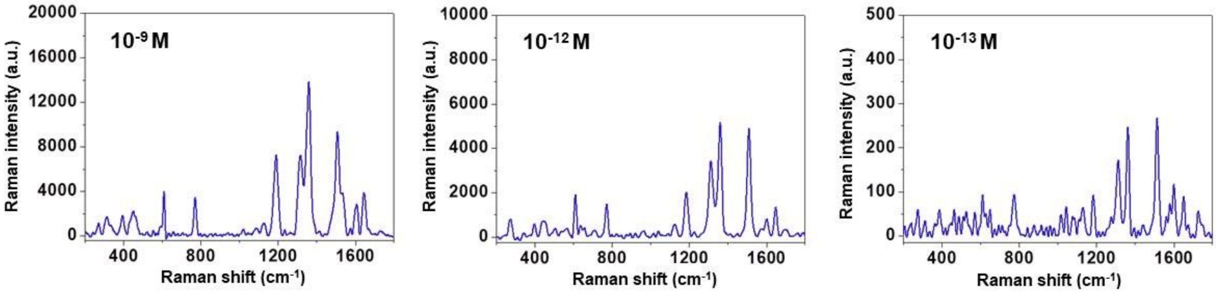

Fig. S5 Raman spectra of R6G from solutions with different concentration at 785 nm excitation wavelength on inverted pyramids SERS device (10 s exposure time, power 9 mW).

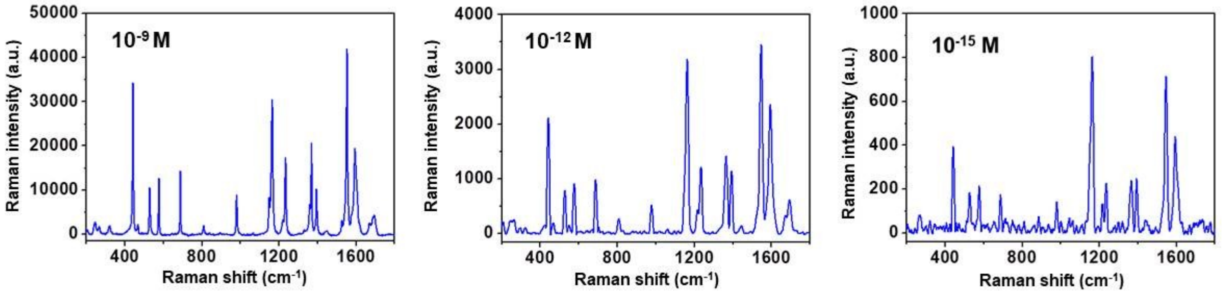

Fig. S6 Raman spectra of coumarin from solutions with different concentration at 785 nm excitation wavelength on inverted pyramids SERS device (10 s exposure time, power 9 mW).

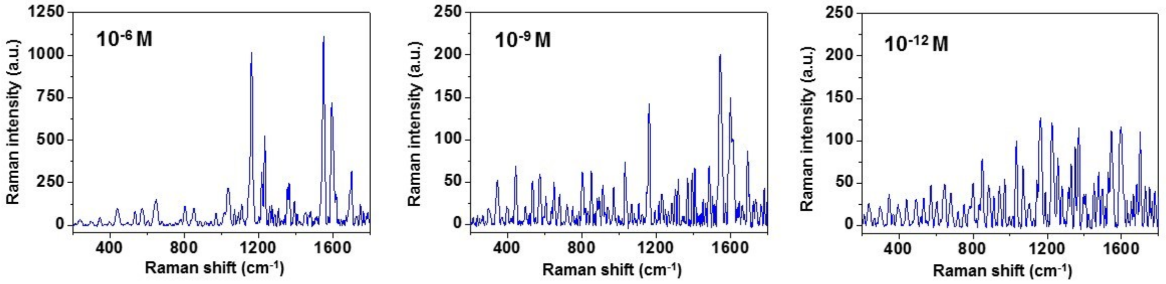

Fig. S7 Raman spectra of coumarin from solutions with different concentration at 514 nm excitation wavelength on positive pyramids SERS device (10 s exposure time, power 0.09 mW).

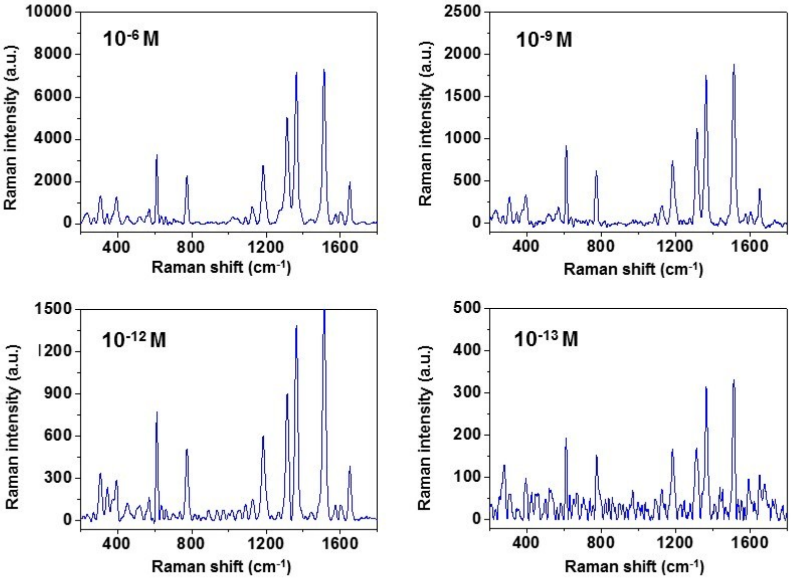

Fig. S8 Raman spectra of R6G from solutions with different concentration at 785 nm excitation wavelength on positive pyramids SERS device (10 s exposure time, power 9 mW).

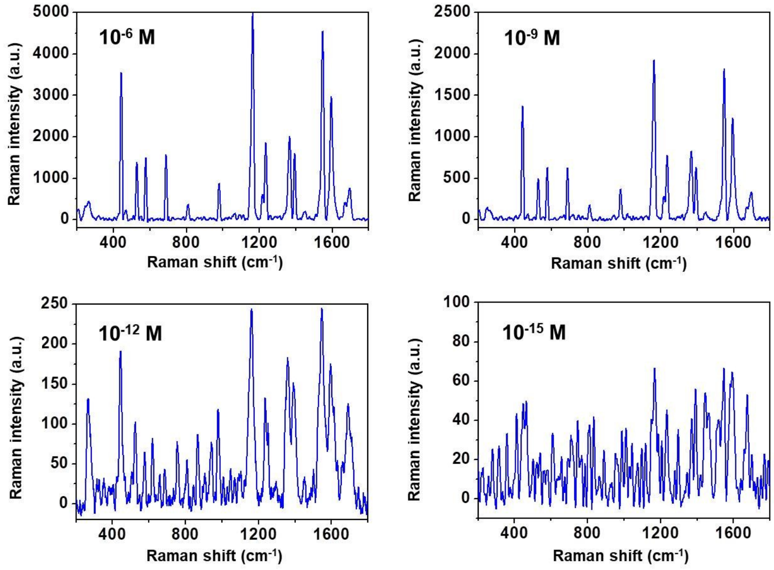

Fig. S9 Raman spectra of coumarin from solutions with different concentration at 785 nm excitation wavelength on positive pyramids SERS device (10 s exposure time, power 9 mW).

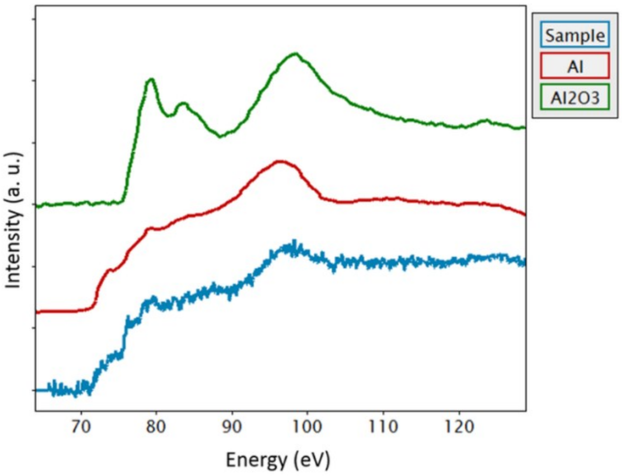

Fig. S10 Core-loss EELS signal of the Al $L_{2,3}$ edge acquired with EELS from the sample compared with $L_{2,3}$ edges of standard metallic Al and Al_2O_3. The fine structure of the signal acquired from the sample is clearly different from that of Al_2O_3 but closely matches that of Al, indicating that the oxide layer thickness in the sample is negligible.